Using fence pulses to suppress stimulated Raman scattering effect in laser–plasma interaction

Yuliang Zhou (周煜梁)[1,2], Zhan Sui (隋 展)[2], Yuanchao Geng (耿远超)[2], Lixin Xu (许立新)[1*], and Hai Ming (明 海)[1]

[1]*Department of Optics and Optical Engineering, University of Science and Technology of China, Hefei 230026, China*

[2]*Research Center of Laser Fusion, China Academy of Engineering Physics, Mianyang 621900, China*

[*]*Corresponding author: xulixin@ustc.edu.cn*

Received May 3, 2014; accepted June 11, 2014; posted online August 22, 2014

In inertial confinement fusion, the laser–plasma interaction (LPI) happens when the high-energy laser irradiates on the target where the scattered light share generated from the stimulated Raman scattering (SRS) effect is difficult to suppress. We propose a method using fence pulses (FPs) to suppress the backward SRS by inhibiting the growth of the intensity of electron plasma waves. Based on our simulation, the FPs can weaken SRS effect in the LPI effectively.

OCIS codes: 290.1350, 290.5910.

doi: 10.3788/COL201412.092902.

In the inertial confinement fusion, either directly or indirectly driven, sufficient laser energy coupled onto the target to create the appropriate conditions for the fusion is required. However, in the coupling process, the stimulated Raman scattering (SRS)[1] and stimulated Brillouin scattering effects in the laser–plasma interaction (LPI) will reduce the laser coupling efficiency. To improve the coupling efficiency of the beam, several beam smoothing methods have been proposed such as smoothing by spectral dispersion (SSD)[2–4], polarization smoothing (PS)[5], and continuous phase plates (CPP)[6]. These methods make the spatial energy distribution of the focal spot[7] on the target surface become more uniform; however, based on experimental results from National Ignition Facility[8], SRS effect still produces large amount of backward scattered light[9–11].

The growth rate of SRS is closely related to laser energy density. SSD, PS, and CPP methods shape the spatial energy distribution to smoothen the laser field intensity on the target surface so that the amount of backward scattered light can be reduced. Here, we propose a new method to suppress SRS backward scattering with the fence pulses (FPs). As the strength of the SRS effect is always changing with the variation of the electron plasma waves (EPWs), this method uses the collision and Landau damping generated by plasma itself to weaken the intensity of EPW during LPI, thus the SRS backward scattered light is reduced. Compared with spatial smoothing methods, the FP method is a time suppression method.

Here we give a brief introduction of the SRS theoretical model, the design of FP, the impact on SRS effect after we add extra frequency modulation to FP and then conclude this study.

To study the temporal evolution of LPI, we choose to use one-dimensional $(x - t)$ fluid simulation model. To have a better understanding of the impact of the pulse of the SRS effects, we only consider the main pulse, SRS, and the EPW three-wave coupling effect in LPI. Electric field between them can be described by[12,13]

$$\left(\frac{\partial}{\partial t}+\frac{c^2k_0}{\omega_0}\frac{\partial}{\partial x}+\gamma_0\right)E_0=-\frac{k_\mathrm{p}}{4}\frac{e}{m_\mathrm{e}\omega_\mathrm{S}}E_\mathrm{S}E_\mathrm{P}, \tag{1}$$

$$\left(\frac{\partial}{\partial t}-\frac{c^2k_\mathrm{S}}{\omega_\mathrm{S}}\frac{\partial}{\partial x}+\gamma_\mathrm{S}\right)E_\mathrm{s}=\frac{k_\mathrm{P}}{4}\frac{e}{m_\mathrm{e}\omega_0}E_0E_\mathrm{P}^{*}, \tag{2}$$

$$\left(\frac{\partial}{\partial t}+\frac{3\upsilon_{\mathrm{th}}{}^2k_\mathrm{P}}{\omega_\mathrm{P}}\frac{\partial}{\partial x}+\gamma_\mathrm{P}\right)E_\mathrm{p}=\frac{k_\mathrm{P}}{4}\frac{e\omega_\mathrm{p}}{m_e\omega_0\omega_\mathrm{S}}E_0E_\mathrm{S}^{*}, \tag{3}$$

where c is the speed of light; ω_0, ω_S, and ω_P are the wave frequencies of the main pulse, SRS scattered light, and the EPW, respectively; k_0, k_S, and k_P represent the wave vectors of the three waves; γ_0, γ_S, and γ_P represent the damping terms of three waves in the plasma; e and m_e represent the charge and mass of electron, and υ_{th} represents the thermal velocity of electron. When the FPs are coupled to the plasma, there is a zero laser energy between two sub-pulses of the FP and the EPW equation takes a simplified form in this time instant given by

$$\left(\frac{\partial}{\partial t}+\frac{3V_{\mathrm{th}}{}^2k_\mathrm{P}}{\omega_\mathrm{P}}\frac{\partial}{\partial x}+2\gamma_\mathrm{P}\right)E_\mathrm{P}=0. \tag{4}$$

From Eq. (4) we can see that the EPW decays with time, the attenuation strength is related to the damping of the EPW which is determined by the temperature and density of the plasma (Fig. 1(a)), and its value is given as

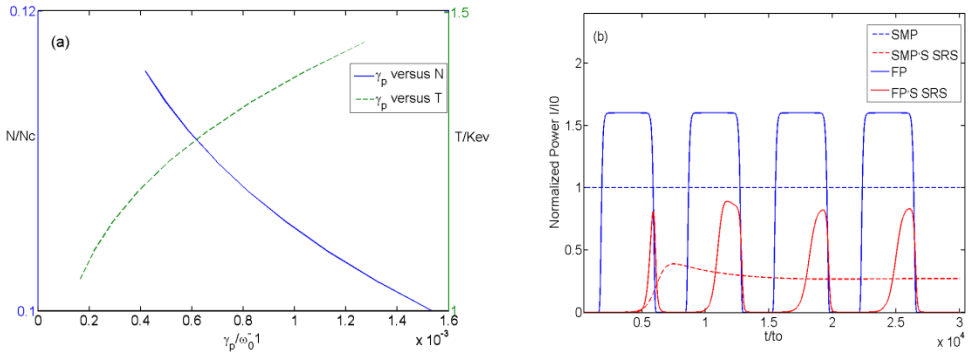

Fig. 1. (a) Change in temperature and density of the plasma and (b) SRS backward scattered light of SMP and the FP.

$$\gamma_{\mathrm{P}} = \upsilon_{\mathrm{ei}}/2 + \gamma_{\mathrm{lan}}, \tag{5}$$

where υ_{ei} and γ_{lan} represent the electron–ion collision damping and Landau damping, respectively, whose expressions are

$$\gamma_{\mathrm{lan}} = \sqrt{\frac{\pi}{8}}\frac{\omega_{\mathrm{p}}}{k_{\mathrm{P}}^{3}\lambda_{\mathrm{D}}^{3}}\left(-\frac{3}{2}-\frac{1}{2k_{\mathrm{P}}^{2}\lambda_{\mathrm{D}}^{2}}\right), \tag{6}$$

$$\upsilon_{\mathrm{ei}} = \frac{4}{3}\frac{(2\pi)^{1/2}e^{4}n_{0}\ln\Lambda}{(kT_{\mathrm{e}})^{3/2}m_{\mathrm{e}}^{1/2}}, \tag{7}$$

$$\ln\Lambda = 7.1 - 0.5\times\ln\left(\frac{n_{0}}{10^{21}}\right) + \ln\left(\frac{T_{\mathrm{e}}}{10^{3}}\right),$$

where λ_{D} is the Debye length. In the simulation n_{c} means critical density and t_{0} means the period of the laser wave.

When using the FP, first we consider the sub-pulse's shape. If the pulse shape has an uneven profile, the corresponding power density is not constant. If the power density is high, then the gain of the EPW will increase very fast which is not conducive to weaken the SRS effect. Second, because the FP we used consists of short pulses, if the sub-pulse's rise time or fall time is too large, when the pulses may overlap, the bottom power density can rise very easily, such as Gaussian FP. Based on these points, we finally choose super-Gaussian pulses as FP short sub-pulses whose rise time and fall time is short so the bottom power density will not increase, and power of the peak has a flat top and a very uniform distribution.

We compare and simulate the SRS backward scattered light of sinusoidal frequency modulation pulse (SMP)[14] and the FP at a constant temperature and uniform plasma. The plasma temperature is 1.5 keV, the plasma density is $0.1n_{\mathrm{c}}$, wavelength λ of the pulses center is 351 nm, interaction time is 30,000 optical cycles, plasma length is 1000λ, $k_{\mathrm{P}}\lambda_{\mathrm{D}}$ is 0.256, average incident intensity of two kinds of pulses is 3 PW/cm^2, SMP modulation frequency is 17 GHz, the modulation width is 150 GHz (before frequency conversion), width of the sub-pulse of the FP is 5 ps, and interval time between each sub-pulses is 3 ps (Fig. 1(b)). From the SRS scattering situation shown in Fig. 1(b), when SMP pulse is used, SRS backward scattered light share is 27%, if FP is used, the SRS backward scattered light share is only 20%. According to the SMP (dotted line), backward scattered light share will not change in a certain time because after pulse interacts with plasma for enough time, EPW saturates and the entire process is in a steady state. Using the FP, when the input energy is 0, collisions and Landau damping efficiently attenuate the EPW and this breaks the saturation state of EPW which means FP shortens the time for the EPW to reach its saturation state. Although SRS peak power of each sub-pulse of FP is larger than that of long pulse, the growth rate will be faster than that in the case of SMP, but SRS from each short pulse grows up from zero, this extends SRS growth time and weakens SRS backward scattered light share in another way.

FP has a very important parameter, that is, the duty cycle. When pulse width of the selected pulse is fixed, the duty cycle determines time interval between each sub-pulses and also the peak power level when the average incident power is fixed. Figure 2 shows the change of SRS backward scattered share when 5 ps sub-pulses have different duty cycle. From Fig. 2 one can find that when the duty cycle increases, time interval between each sub-pulse becomes short, and the EPW cannot be attenuated effectively. Although the peak power density of the sub-pulse is lowered at the

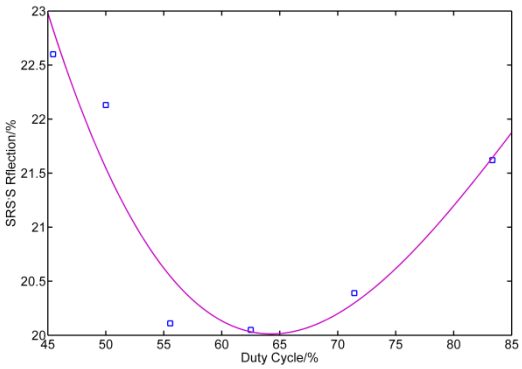

Fig. 2. SRS backward scattered light share with different duty cycles.

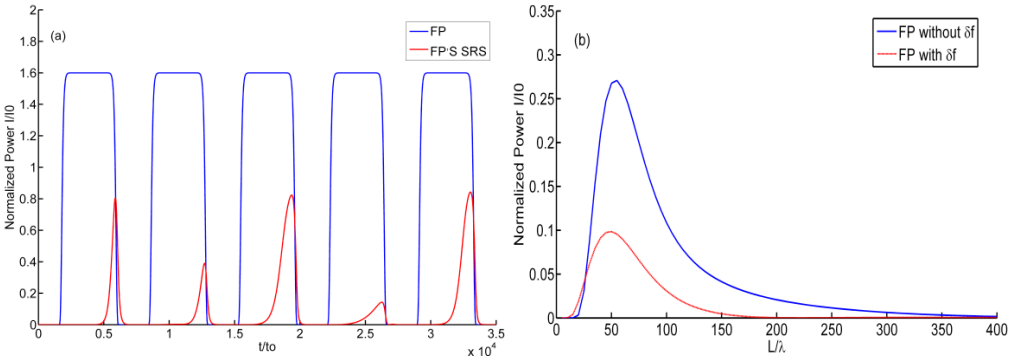

Fig. 3. (a) FP and its backward scattered light situation with the frequency difference and (b) full-space distributions of EPW on the falling edge of a short pulse from FP.

same time, SRS reflection share is still high, relative to a not large SMP attenuation. When we reduce the duty cycle of the sub-pulse, time interval also increases, corresponding sub-pulse's peak power grows which makes the growth of SRS in sub-pulses become faster. Figure 2 shows that the duty cycle has an optimal value. In our simulation, when sub-pulse width is 5 ps in FP and the duty cycle is set at 65%, we have the lowest share of SRS backward scattered light.

FP can reduce SRS backward scattered light share by changing the state of the EPW. From Fig. 1(b), SRS backward scattered light share of a single short pulse is still high which is due to the increase in the short-pulse power density. Since the interval time is 3 ps which is too short for the EPW to decay to a satisfactory level, density perturbations caused by the previous pulse still have a bad effect on the next pulse. In order to weaken the influence on a pulse caused by the previous one, we make two adjacent short pulses have a certain difference in the central frequency. So when the EPW from the previous pulse affects the next one, due to the mismatch of the central frequencies, the increase in EPW will be slowed down, so the SRS backward scattered light share can be further attenuated. We simulate the incident light and backward scattered light situation with the frequency difference (Fig. 3), the parameters we used is the same as in Fig. 1, the only difference is that between two adjacent pulses the frequency difference is 250 GHz (before frequency conversion).

By comparing Figs. 3(a) and 1(b) we can say that with the frequency difference, backward scattered light share of FP is reduced significantly and each short pulse's backward scattered light share is reduced as well. Among the short pulses, backward scattered light share of the ones with frequency difference are reduced the most. Because of the frequency difference, effect on the pulse caused by the EPW from the previous pulse is greatly weakened. Figure 3(b) shows the full-space distributions of EPW on the falling edge of a short pulse from FP with and without the frequency difference. We can see that the growth of EPW intensity is significantly inhibited.

Figure 4 shows the SRS backward scattered light share from FP or SMP interacts with uniform plasma at different temperatures. The plasma density is $0.1n_c$, temperature varies from 1.5 to 1.6 keV. Width of the short pulses from FP is 5 ps, pulse interval is 3 ps, and corresponding center frequency difference is 250 GHz. From Fig. 4 we can see that, compared with result from SMP, FP with different frequency can reduce the SRS share to a great extent. When temperature is between 1.5 and 1.6 keV, most corresponding SRS share dropped to less than 5%.

In conclusion, we present a new method to reduce the SRS effect in LPI using FP consisting of a series of super-Gaussian short pulses. When FP interacts with plasma, the EPW is attenuated between the sub-pulses, so the SRS backscattered light share is weakened. This share can reduce most of the value under the optimal duty cycle. If two adjacent sub-pulses are made to have a different frequency, the SRS scattered share can weaken further. When the frequency difference is 250 GHz, the SRS back scattered light share is greatly reduced which is satisfactory.

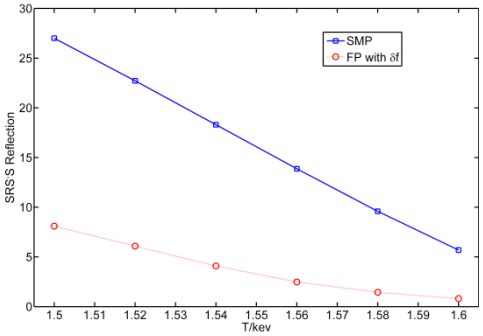

Fig. 4. SRS backward scattered light share from FP or SMP.

References

1. M. V. Goldman and D. F. D. Bois, Phys. Fluids **8,** 1404 (1965).
2. S. Skupsky, R. W. Short, T. Kessler, R. S. Craxton, S. Letzring, and J. M. Soures, J. Appl. Phys. **66,** 3456 (1989).

3. Y. Jiang, X. Li, S. Zhou, W. Fan, and Z Lin, Chin. Opt. Lett. **11,** 052301 (2013).
4. Y. Jiang, S. Zhou, R. Wu, J. Li, X. Li, and Z. Lin, Chin. Opt. Lett. **11,** 081404 (2013).
5. D. H. Munro, S. N. Dixit, A. B. Langdon, and J. R. Murray, Appl. Opt. **43,** 6639 (2004).
6. S. N. Dixit, M. D. Feit, M. D. Perry, and H. T. Powell, Opt. Lett. **21,** 1715 (1996).
7. J. E. Rothenberg, J. Opt. Soc. Am. B **14,** 1664 (1997).
8. C. A. Haynam, P. J. Wegner, J. M. Auerbach, M. W. Bowers, S. N. Dixit, G. V. Erbert, G. M. Heestand, M. A. Henesian, M. R. Hermann, K. S. Jancaitis, K. R. Manes, C. D. Marshall, N. C. Mehta, J. Menapace, E. Moses, J. R. Murray, M. C. Nostrand, C. D. Orth, R. Patterson, R. A. Sacks, M. J. Shaw, M. Spaeth, S. B. Sutton, W. H. Williams, C. C. Widmayer, R. K. White, S. T. Yang, and B. M. V. Wonterghem, Appl. Opt. **46,** 3276 (2007).
9. D. H. Froula, L. Divol, R. A. London, R. L. Berger, T. Doeppner, N. B. Meezan, J. Ralph, J. S. Ross, L. J. Suter, and S. H. Glenzer, LLNL-JRNL 420444 (2009).
10. D. E. Hinkel, M. D. Rosen, E. A. Williams, A. B. Langdon, C. H. Still, D. A. Callahan, J. D. Moody, P. A. Michel, R. P. J. Town, R. A. London, and S. H. Langer, Phys. Plasmas **18,** 056312 (2011).
11. S. W. Haan, J. D. Lindl, D. A. Callahan, D. S. Clark, J. D. Salmonson, B. A. Hammel, L. J. Atherton, R. C. Cook, M. J. Edwards, S. Glenzer, A. V. Hamza, S. P. Hatchett, M. C. Herrmann, D. E. Hinkel, D. D. Ho, H. Huang, O. S. Jones, J. Kline, G. Kyrala, O. L. Landen, B. J. MacGowan, M. M. Marinak, D. D. Meyerhofer, J. L. Milovich, K. A. Moreno, E. I. Moses, D. H. Munro, A. Nikroo, R. E. Olson, K. Peterson, S. M. Pollaine, J. E. Ralph, H. F. Robey, B. K. Spears, P. T. Springer, L. J. Suter, C. A. Thomas, R. P. Town, R. Vesey, S. V. Weber, H. L. Wilkens, and D. C. Wilson, Phys. Plasmas **18,** 051001 (2011).
12. D. W. Forslund, J. M. Kindel, and E. L. Lindman, Phys. Fluids **18,** 1002 (1975).
13. R. L. Berger, B. F. Lasinski, T. B. Kaiser, E. A. Williams, A. B. Langdon, and B. I. Cohen. Phys. Fluids B **5,** 2243 (1993).
14. D. Xu, J. Wang, M. Li, H. Lin, R. Zhang, Y. Deng, Q. Deng, X. Huang, M. Wang, L. Ding, and J. Tang, Opt. Express **18,** 6621 (2010).